BULLETIN OF THE POLISH ACADEMY OF SCIENCES
TECHNICAL SCIENCES, Vol. 71(6), 2023, Article number: e147347
DOI: 10.24425/bpasts.2023.147347

Comparison of the effects of anthropogenic seismic events and natural earthquakes on buried infrastructure network components

Janusz RUSEK[1]*, **Leszek SŁOWIK**[2], and **Krzysztof TAJDUŚ**[1]

[1] AGH University of Krakow al. Adama Mickiewicza 30, 30-059 Krakow, Poland
[2] ITB Building Research Institute ul. Filtrowa 1, 00-611 Warsaw, Poland

Abstract. Mining tremors may have an impact on the safety risk of steel pipelines through their effects. It is therefore important to quantify the impact of a high-energy mining tremor in terms of strength. In addition, a comparison of the results obtained with the effect of a seismic tremor can illustrate the scale of such a hazard. Recently, this has been a very frequently raised issue in the area of surface protection against negative mining impacts and the protection of post-mining areas. Ensuring safe use is particularly important for gas transmission elements. This paper presents the results of a comparative analysis of the impact of mining tremors and seismic impacts on a specimen steel pipeline segment. The analyzed pipeline is located in the eastern part of Poland in the area of paraseismic impacts of the LGCD (Legnica-Glogow Copper District) mine. For this purpose, an analytical approach was used to assess the impact of seismic wave propagation on underground linear infrastructure facilities. Accelerogram records for the 02-06-2023 seismic tremor from Turkey and the mining tremor for 11-25-2020 were used. In the case of the design of underground pipelines, the cross-section of the element for which measures describing wall stress and the ovalization of the cross-section are determined is usually considered. In the situation of the influence of seismic wave propagation or so-called permanent ground deformation, the response of the pipeline in the longitudinal direction is analyzed. As a final result, longitudinal strains transferred to the pipeline as a consequence of the propagating seismic wave and mining tremor were determined. The absolute difference between the deformations in the ground and along the length of the pipeline was determined. This type of analysis has not been carried out before and provides new insights into the topic of paraseismic impacts on the scale of their interaction with natural earthquakes. Mining tremor data was obtained from the mine's seismological department. The seismic tremor data, on the other hand, was downloaded via the publicly available ESM (Engineering Strong-Motion Database).

Key words: pipeline; dynamic; seismic; mining.

1. INTRODUCTION

The issue of seismic hazards is widespread around the world, especially in areas where such natural phenomena occur [1, 2]. Phenomena of a similar nature but of lower intensity also occur in areas affected by underground mines. One of the results of mining exploitation is the continuous deformation of the mining area [3–6], accompanied by mining tremors taking place during the works [7–11].

To this date, there have been lots of studies on the effects of mining tremors on above-ground civil structures, in which, due to their design, the forcing of the tremor induces additional inertial forces [12–14]. A similar state of affairs applies to the determination of the dynamic response of underground structures. Also in the case of Polish mining sites, there are works referring to this theme [15]. However, there are still no studies showing a comparison of the effects from seismic and mining tremors on pipelines. The world literature, in the form of monographs, standards and guidelines, focuses mainly on the impact of natural phenomena [16–18]. Studies on the impact of natural earthquakes on underground structures are considered in terms of seismic wave propagation in the ground [19–21] and the impact of the so-called permanent ground deformation (PGD) [22–24]. Within the framework of this study, an attempt was made to estimate the impact of mining tremors on steel utility pipelines, in terms of the propagation of a paraseismic interaction wave in the ground. In this case, it was considered that the only possible solution to the problem of mining tremor impacts on underground utilities was to adapt existing directives applicable to seismic areas [18, 25, 26]. For the calculation of underground pipelines at the design stage, analytical methods are most often used to assess the deformation and strength of the pipeline cross-section [27]. However, seismic analysis mainly considers the longitudinal direction of the pipeline, for which instantaneous deformations and curvatures are determined [26]. Thus, the analytical solutions used to assess the impact of propagating waves induced by earthquakes were transferred and applied to the field of anthropogenic impacts generated by underground mining exploitation. It should be mentioned that in addition to the analytical approach, spatial FEM modelling of pipelines subjected to natural earthquake impacts was also used. [28, 29]. Due to the utilitarian nature of the work, the focus was on a simplified approach.

*e-mail: rusek@agh.edu.pl

Manuscript submitted 2023-07-06, revised 2023-09-11, initially accepted for publication 2023-09-25, published in December 2023.

In addition to the main purpose of the research undertaken, which was to identify a procedure to assess the impact of ground vibrations induced by underground mining on existing buried pipelines, an additional scientific problem was posed. Namely, it was also considered important to demonstrate the difference quantitatively, by comparing the results obtained for a mining tremor with natural phenomena of distinctly higher intensity. In conclusion, the specific objective of this study was to determine the difference between the effect of mining tremors and high-energy earthquakes. For this reason, in order to ensure that the stated aim of the research is met, in addition to providing a simplified procedure for assessing the impact of mining tremors on existing underground pipelines, the case of seismic wave propagation recorded for an earthquake in the province of Gaziantep, Turkey (02-06-2023 [30, 31]) was also analyzed. The data was extracted from the publicly available ESM database (Engineering Strong-Motion Database). The mining tremor, on the other hand, was downloaded from the mine catalogue and took place on the LGCD (Legnica-Glogow Copper District) mining terrain (11-25-2020) [32].

This paper is intended to fill in the gaps in the subject of the impact of paraseismic tremors on underground pipelines. In addition, it will show the difference of such an impact when confronted with a high-energy seismic event. This may contribute to more conscious actions with regard to planned protection or retrofitting.

2. RESEARCH METHODOLOGY

Many studies on the effects of earthquakes on structures [26], particularly underground pipelines, use a simplified methodology based on the solutions of the Newmark model [33]. This determines the deformations in the ground that can be transmitted to the pipeline during the movement of the seismic wave. According to [26], the material transverse waves (**S**) and surface Rayleigh waves (**R**) have a real effect on pipeline strain. The peak velocity (PGV) and ground accelerations (PGA) recorded at the surface are also relevant here. From this, relationships are obtained that allow the determination of longitudinal deformations in the ground in the pipeline neighborhood (1) as well as of curvatures [17]. Figure 1 presents an overview schema of relationship (1).

$$\varepsilon_g = \frac{\mathrm{PGV}}{V_S} \sin\emptyset \cos\gamma_S \,, \tag{1}$$

where: PGV peak value of vibration velocity of ground particles at the surface V_S velocity of propagation of shear S-wave γ_S angle between wave propagation direction and horizontal plane $\emptyset$ angle between wave propagation direction and vertical plane.

In the case of determining the value resulting from relation (1), seismological information on the velocity model of transverse **S**-wave versus depth [34] or the averaged V_{S30} value [35] can be used. According to [26], relationship (1) can be reduced to form (2).

$$\varepsilon_g = \frac{\mathrm{PGV}}{2V_S} \,. \tag{2}$$

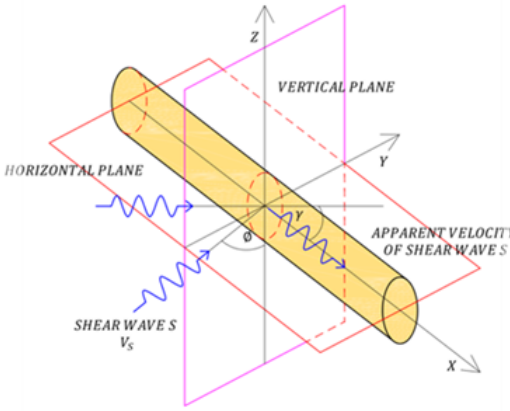

Fig. 1. An overview schema of relationship (1)

The effect of the Rayleigh surface wave (V_R) propagation is included in relation (3) [26].

$$\varepsilon_g = \frac{\mathrm{PGV}}{V_R} \,, \tag{3}$$

where: V_R apparent velocity of propagation of surface wave R.

Here, it is problematic to determine the apparent velocity of the propagating surface wave R expressed by variable V_R. This value can be determined in at least three ways. The first is to use the relationship between V_R and V_S velocities taking into account Poisson's coefficient (4). This is the analytical solution used for wave propagation issues in an elastic medium [36].

$$\frac{V_R}{V_S} = \frac{0.87 + 1.12\mu}{1 + \mu} \,, \tag{4}$$

where: μ Poisson's coefficient.

The second way is to apply explicitly the arrangements contained in [18, 25]. These determine the value of the apparent seismic wave velocity at arbitrary levels equal to 2000 m/s [25] and 500 m/s [18].

The third method is based on the assumption that the approximation of the apparent velocity of a surface wave V_R is the so-called phase velocity (C_{ph}). In this case, so-called dispersion curves are used. These allow the phase velocity of a V_R surface wave to be indicated in the frequency domain. Dispersion curves can be determined either by means of MASW (Multi-Channel Analysis of Surface Wave) measurements [37] or by approximation [26, 38]. For the calculations in this paper, the dispersion curve approximation method was used, which is described in detail in [38].

An additional form of seismic wave propagation manifestation in underground pipelines is curvature, which can translate into structural strength. The curvature is the result of peak ground acceleration and the velocity of the propagating **S**-wave [26]. In reality, however, the impact of curvature is negligible and was therefore not included in further analyses.

In reality, however, only a certain proportion of the originally determined impact is transmitted to the pipelines. In order to determine the actual value of the pipeline strain (ε_P), according

to [39], it is necessary to make a transition from the value of ε_g using the reduction relation (5).

$$\varepsilon_p = \beta_c \cdot \varepsilon_g \,, \tag{5}$$

where: β_c *conversion factor*.

$$\beta_c = \begin{cases} 1 & \text{if } \gamma_{cr} \geq \gamma_0 \,, \\ \dfrac{1}{\dfrac{\gamma_{cr}}{\gamma_0} \cdot \left(1 + \left(\dfrac{2\pi}{\alpha}\right)^2 \cdot \dfrac{AE}{K_g}\right)} \cdot q & \text{if } \gamma_{cr} < \gamma_0 \,, \end{cases} \tag{6}$$

where:

$\gamma_{cr} = \dfrac{t_u}{\pi DG}$, $\gamma_0 = \dfrac{2\pi}{\alpha}\dfrac{Et}{G}\varepsilon_g\beta_0$,

$t_u = \pi D\overline{\gamma}H\left(\dfrac{1+k_o}{2}\right)\tan k\emptyset_S$, $K_g = 2 \cdot \pi \cdot G$

c_p heat capacity, J/(kg·K)

γ_{cr} critical shear strain

γ_0 maximum shear strain at pipe-soil interface

t_u maximum longitudinal force per unit length at soil-pipe interface

D pipe diameter

G shear modulus of soil

α wavelength

q factor that ranges from 1 to $\pi/2$ and quantifies the degree of slippage at the pipe-soil interface

t pipe wall thickness

A cross-section area of pipe

E elasticity modulus of pipe material

K_g linear soil stiffness per unit length

$\overline{\gamma}$ volumetric weight of soil

H pipeline installation depth

k_o coefficient of lateral soil pressure at rest

k friction reduction factor, ratio of joint eccentricity to wall thickness.

3. RESULTS AND DISCUSSION

The basis for the analyses was a 300-meter segment of a steel pipeline with a diameter of $D = 300$ mm, located within the influence range of the paraseismic impact of a Polish mine. This phenomenon was recorded on 11-25-2020 in the LGCD mining area. The results obtained were compared with the impact of an earthquake that occurred in Turkey on 02-06-2023 in the area of the city of Gaziantep. This comparison gave an idea of the magnitude of mining tremors and the negative effects they generate on underground infrastructure. The magnitude of the longitudinal deformations that can be transmitted to the analyzed pipeline under dynamic impacts induced by mining activities and natural earthquakes was quantified.

3.1. Analysis of impact of a mining tremor

In order to determine the longitudinal strains in the subject pipeline, the relation described in Chapter 3 and the data from the recordings of the magnitude ML = 4.1 mining tremor were used. The recordings of this phenomenon are presented in the form of velocity and acceleration of ground in time, for three measuring stations labelled A, B and C, respectively. For further analyses, the course of vibrations with the highest intensity in the horizontal plane was selected (registration recorded at station C in horizontal direction E – see Figs. 2 and 3). Peak velocity of the recorded vibrations is PGV = 2.54 cm/s in the case of the analyzed tremor (cf. Fig. 2). In contrast, peak ground particle acceleration reaches PGA = 188 cm/s^2 (cf. Fig. 3).

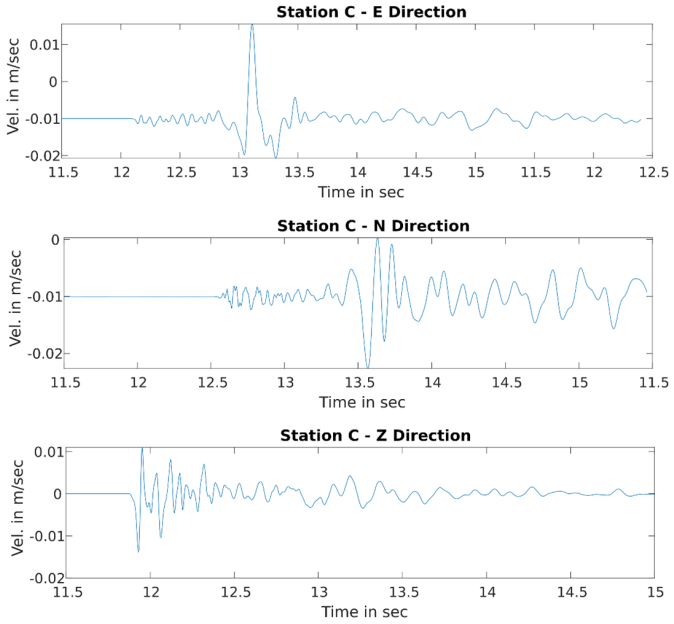

Fig. 2. Time recording of ground velocity at measuring station C (11-25-2020, LGCD mining area)

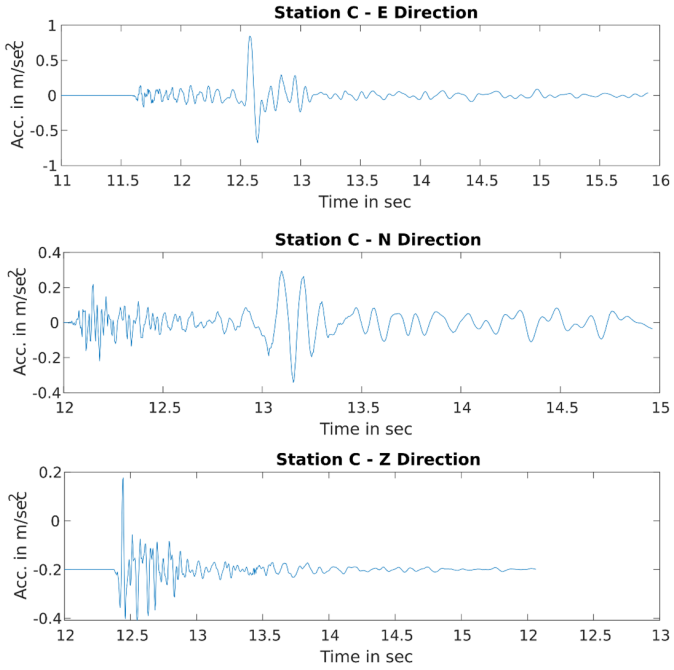

Fig. 3. Time recording of ground accelerations at measuring station C (11-25-2020, LGCD mining area)

Further, based on the registration indicating the highest peak value of ground velocity, a *Fourier* transformation was performed to obtain the frequency spectrum of the signal (cf. Fig. 4). This was necessary in order to determine, in a further step, the value of phase velocity of the Rayleigh wave. Analysis of the spectrum indicated that the peak value of the acceleration is carried by frequency $f = 2.92$ Hz (cf. Fig. 4).

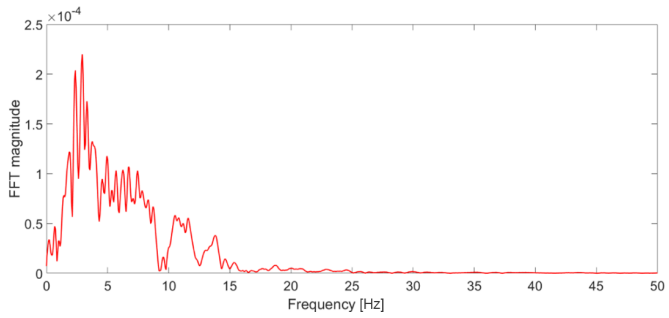

Fig. 4. Frequency spectrum of the C station speed signal

The next step was to determine the longitudinal strains (2) resulting from the propagating tremor. For this purpose, the velocity model of the shear S-wave for the analyzed site was used, the distribution of which is illustrated in Fig. 5 [32]. This was necessary in order to establish the required propagation velocity of the shear S-wave. On the basis of the velocity model, it was determined that at the depth of the pipeline foundation (up to 40 m – cf. Fig. 5), the shear S-wave propagates with a velocity of no more than $V_S = 230$ m/s. On this basis, the longitudinal deformations from the S-wave were determined (7).

$$\varepsilon_g^{\mathbf{S}} = \frac{\mathrm{PGV}}{2V_S} = 0.055\ \mathrm{mm/m}. \tag{7}$$

In the final step, the longitudinal strain from the propagating surface Rayleigh wave was determined according to relation (3). Here, according to [26], it was assumed that the approximation of the apparent velocity V_R could be the phase velocity C_{ph}. This value was determined from an approximate dispersion curve. The scheme for determining this value is presented in Fig. 6. According to the shear wave velocity model S (cf. Fig. 5), three soil layers of the following thicknesses were assumed for the calculations: 40 m ($V_S = 230$ m/s), 60 m ($V_S = 720$ m/s) and the remaining soil below, for which the shear wave velocity was assumed to be $V_S = 920$ m/s.

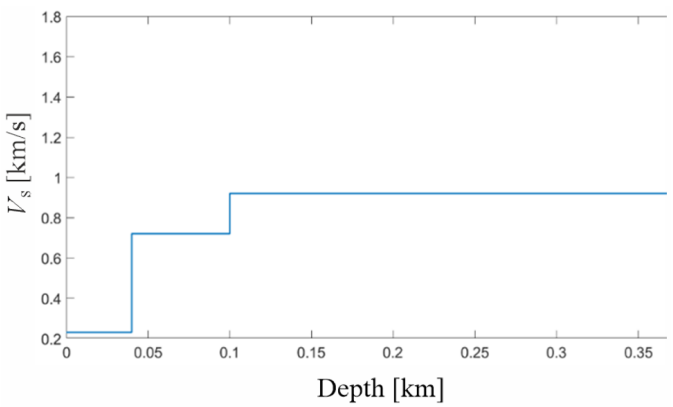

Fig. 5. Velocity model of shear S-wave [32]

$$C_{ph} = \begin{cases} 0{,}875C_H & \text{if } \frac{H_S f}{C_L} \le 0{,}25 \\ 0{,}875C_H - \frac{0{,}875C_H - C_L}{0{,}25}\left(\frac{H_S f}{C_L} - 0{,}25\right) & \text{if } 0{,}25 < \frac{H_S f}{C_L} \le 0{,}5 \\ C_L & \text{if } \frac{H_S f}{C_L} > 0{,}5 \end{cases}$$

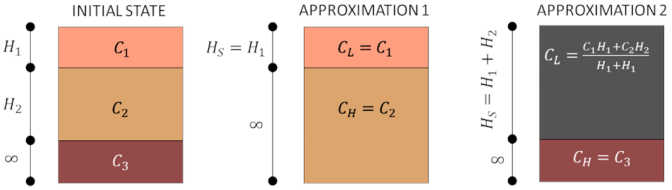

Fig. 6. Schematic of the procedure for determining the dispersion curve for multi-layer soil (based on [26])

Finally, an approximation of the dispersion curve for phase velocity was obtained, which is illustrated in Fig. 7. On this basis, it was possible to determine phase velocity for the predetermined frequency corresponding to the maximum ground acceleration f = 2.92 Hz. The value of phase velocity was set at $C_{ph} = 270$ m/s (cf. Fig. 7). This value was also used for further calculations.

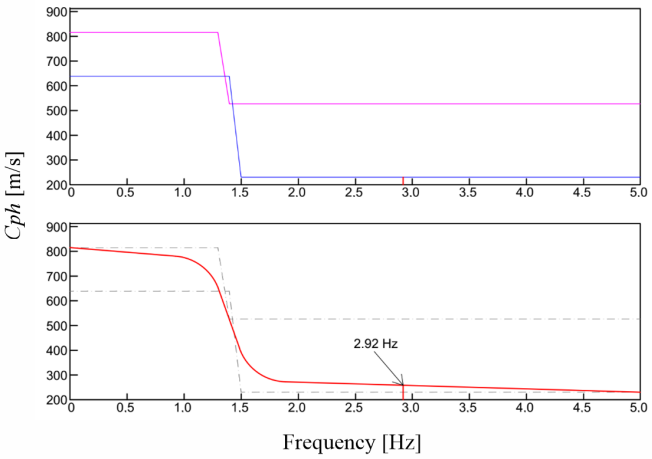

Fig. 7. Determined approximation of the dispersion curve for the adopted multi-layer soil

According to the procedure used, the value of the longitudinal strain in the ground resulting from the propagating Rayleigh surface wave was determined (8). As can be seen, the longitudinal strain in the ground reaches a higher value for this wave than the curvature due to the action of the material S-wave. In contrast, due to the action of the material S-wave, the curvature appears to have a negligible value for further calculations.

$$\varepsilon_g^{\mathbf{R}} = \frac{\mathrm{PGV}}{V_R} \approx \frac{\mathrm{PGV}}{C_{ph}} = 0.094\ \mathrm{mm/m}. \tag{8}$$

Further, taking into account the assumed ground conditions (cf. Table 1), the longitudinal strain in soil ε_g to the strain transferred to the subject pipeline ε_p was reduced. The data summarized in Table 1 represent the parameters that determine friction at the pipeline-ground interface. They relate both to the soil itself and to the material of which the pipeline is made. They are all used in determining the friction or slippage values according to formula (6). According to relation (5) and the assumed ground conditions, a value indicating that there is no slippage on the side of the pipeline and, thus, a reduction value of $\beta_c = 1$, was obtained. This means that the deformation in the ground will be entirely transferred to the pipeline.

Table 1
Strength and geometrical parameters of the soil and pipeline

Volumetric weight of soil	γ	17 kN/m^3
Shear modulus of soil	G	27.8 MPa
Coefficient of lateral soil pressure at rest	k_o	1.0
Friction reduction factor, ratio of joint eccentricity to wall thickness	k	0.8
Equivalent spring constant to reflect soil-structural interaction	K_g	174.61 MPa
Internal friction angle	$\emptyset_S$	20°
Pipeline installation depth	H	1.6 m
Pipe wall thickness	t	10 mm
Wavelength	α	600 m
Elasticity modulus of pipe material	E	205 GPa

3.2. Analysis of impact of a seismic tremor

In order to compare the intensity and negative effects on underground infrastructure, a natural seismic tremor was analyzed in addition to a mining tremor. A phenomenon that occurred on 02-06-2023 and affected the territory of Turkey near the city of Gaziantep [30, 31] was considered here. This tremor was characterized by a magnitude of ML = 7.8 and caused widespread devastation of buildings and the death of many people. There is little information, however, on the damage to underground infrastructure. This makes it all the more important to understand the impact of such a powerful phenomenon on underground linear infrastructure.

On the basis of information taken from [40], in addition to the magnitude of the tremor, the peak values of velocity and acceleration of ground vibrations in the most intense phase of the tremor were also recorded. The recorded velocities and accelerations are presented in Figs. 8 and 9. The values of the obtained vibration parameters are summarized in Table 2. As can be seen, the values of peak ground accelerations match, and in the case of the Z direction, exceed the value of gravitational acceleration. Additionally, in accordance with the methodology adopted in Chapter 3, information on the propagation of a transverse material S-wave at the depth of up to 30 m (V_{S30} = 618 m/s), which is very important from the point of view of the conducted analyses, was obtained [40].

Table 2
Characteristics of the 02-06-2023 tremor near the city of Gaziantep, Turkey

	Direction of propagation		
	E	N	Z
PGA	745.13 cm/s^2	889.70 cm/s^2	1 283.47 cm/s^2
PGV	209.02 cm/s	128.19 cm/s	82.15 cm/s

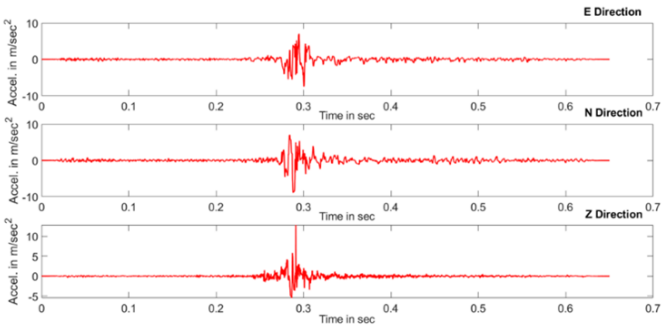

Fig. 8. Time course of ground accelerations in the N, E and Z directions for the tremor of 02-06-2023 near the city of Gaziantep, Turkey

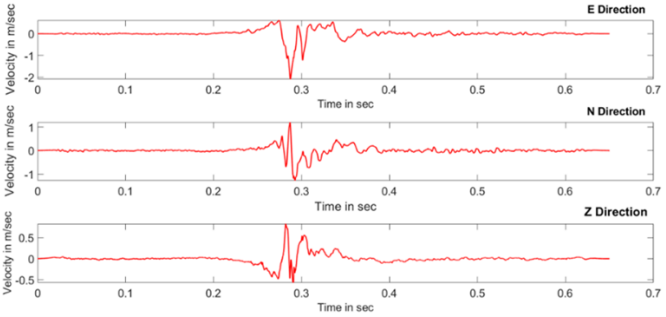

Fig. 9. Time course of ground velocities in the N, E and Z directions for the tremor of 02-06-2023 near the city of Gaziantep, Turkey

With this set of information at one's disposal, one was limited to the determination of longitudinal strains in the ground. In order to use relation (3), it was necessary to determine the velocity of propagation of the Rayleigh surface wave. At this stage, a Poisson's ratio of 0.25 was also assumed. Using formula (3) and relation (4), the desired value of strain (9) was determined.

$$V_R = V_{S30}\frac{0.87 + 1.12\mu}{1+\mu} = 568.6 \text{ m/s}. \tag{9}$$

The determined V_R value and the peak velocity value PGV = 209.02 cm/s allowed the determination of the longitudinal strain in the soil.

$$\varepsilon_g = \frac{PGV}{V_R} = 3.56 \text{ mm/m}. \tag{10}$$

As in the case of the mining tremor analysis, an attempt was made to establish the level of transmission of the obtained strain in the ground to the pipeline. Assuming ground conditions (cf. Table 1) analogous to those of the analyzed mining tremor, and identical geometric and material characteristics of the underground structure, the value of deformation transferred to the pipeline was obtained (11).

$$\varepsilon_p = \beta_c \cdot \varepsilon_g = 0.5696 \text{ mm/m}. \tag{11}$$

As can be seen, according to (11), the longitudinal strains in the soil are subject to a reduction of approximately 85%. This is due to the exceeding of the friction limit and the slippage of the pipeline relative to the surrounding soil.

Table 3 compares the results obtained for the mining tremor and natural earthquake. As can be seen, horizontal deformation in the ground from the mining tremor is only a value of about 3% as compared to the deformation resulting from the earthquake. In contrast, the situation is different for deformations transmitted to the pipeline. Due to the lack of slip in the case of a mining tremor, all of the deformation is transmitted to the pipeline. In the case of a seismic tremor, only some of the deformation from the ground is transmitted to the pipeline. This brings the longitudinal strain in the pipeline from a mining tremor up to 16.5% of the earthquake-generated values.

Table 3

Comparison of the resulting ground and pipeline deformation values for mining tremor and natural earthquake

Mining tremor		Earthquake	
Ground strains	Pipeline strains	Ground strains	Pipeline strains
0.094 mm/m	0.094 mm/m	3.56 mm/m	0.570 mm/m

The results summarized in Table 3 show that the impact of mining tremors is noticeable given the reference scale of pipeline deformation resulting from a mining tremor.

From the analysis of both events, it is evident that the ground strains caused by the tremor reach maximum values in the case of the Rayleigh surface wave propagation. This is in agreement with the literature on the subject. It has also been shown that the longitudinal strain in the ground for a mining tremor is approximately 40 times smaller than for a very intense mining tremor. This relationship is only a rough estimate and multiscale studies need to be undertaken to establish the true relationship, taking into account a much larger number of cases. It is interesting to note that in the case of a mining tremor, there is no cutting at the ground-pipeline interface, resulting in all of the longitudinal strain from the ground being transferred losslessly to the object. The situation is different in the case of the seismic tremor analyzed, where the reduction reaches about 85% of the input value. It follows that, while the deformation in the ground from a mining tremor is much smaller than in the case of a natural phenomenon, the difference in the deformation values of the pipeline itself is distinctly smaller (the effect from a seismic tremor is six times greater than the effect from a mining tremor).

4. CONCLUSIONS

In this study, an example of a steel pipeline segment was analyzed, which was loaded by a mining tremor and a tremor from a natural earthquake. The mining tremor was characterized by ground vibrations with the following peak values: velocity PGV = 2.54 cm/s and accelerations PGA = 188 cm/s^2. In contrast, the seismic tremor that was recorded on 02-06-2023 in the city of Gaziantep, Turkey, was characterized by peak ground velocity of PGV = 209.02 cm/s and an acceleration of PGA = 1 283.47 cm/s^2.

The study compared the effects of a typical mining tremor and a high-energy seismic event. The result of this comparison was that, although seismic tremors generate much higher values of deformation in the ground, pipeline deformation due to mining tremors is about 15% of its value. Thus, mining tremors can have a non-negligible effect on the use of these types of building structures. The results obtained therefore indicate that the scope of research should be broadened, using both advanced FEM tools and continuous monitoring of underground pipeline damage in seismic areas. The latter should provide the data necessary to determine the risk of damage due to single or multiple seismic events in mining areas. Such a research plan can lead to more accurate decisions on securing or upgrading existing underground networks.

The analyses carried out also show the necessity of measuring and publishing the results of the Rayleigh surface wave propagation. This applies to mining areas but also to those exposed to seismic events. Archiving such data can be helpful, as shown in the body of this work, for relatively easy and quick estimation of dynamic influences on underground utility networks.

REFERENCES

[1] K.S. Hudson, M.B. Hudson, J. Hu, A. Harounian, and M. Lew, "Quantifying Earthquake Hazards to Lifeline Systems at a Regional Scale with a Study of the Los Angeles Water System Pipeline Network," in *Lifelines 2022*, 2022, pp. 428–439.

[2] N.S. Kwong, K.S. Jaiswal, J.W. Baker, N. Luco, K.A. Ludwig, and V.J. Stephens, "Earthquake Risk of Gas Pipelines in the Conterminous United States and Its Sources of Uncertainty," *ASCE-ASME J. Risk. Uncertain. Eng. Syst. Part A.-Civ. Eng.*, vol. 8, no. 1, p. 4021081, 2022, doi: 10.1061/AJRUA6.0001202.

[3] Z. Jing, J. Wang, Y. Zhu, and Y. Feng, "Effects of land subsidence resulted from coal mining on soil nutrient distributions in a loess area of China," *J. Clean Prod.*, vol. 177, pp. 350–361, 2018, doi: 10.1016/j.jclepro.2017.12.191.

[4] K. Tajduś, R. Misa, and A. Sroka, "Analysis of the surface horizontal displacement changes due to longwall panel advance," *Int. J. Rock Mech. Min. Sci.*, vol. 104, pp. 119–125, 2018, doi: 10.1016/j.ijrmms.2018.02.005.

[5] K. Tajduś *et al.*, "Analysis of Mining-Induced Delayed Surface Subsidence," *Minerals*, vol. 11, no. 11, p. 1187, 2021, doi: 10.3390/min11111187.

[6] L. Szojda and Ł. Kapusta, "Numerical Analysis of Buildings Located on the Edge of the Post-Mining Basin," *Arch. Min. Sci.*, vol. 68, no. 1, pp. 125–140, 2023, doi: 10.24425/ams.2023.144321.

[7] P. Boroń, J.M. Dulińska, and D. Jasińska, "Impact of High Energy Mining-Induced Seismic Shocks from Different Mining Activity Regions on a Multiple-Support Road Viaduct," *Energies*, vol. 13, no. 16, p. 4045, 2020, doi: 10.3390/en13164045.

[8] E. Pilecka, K. Stec, J. Chodacki, Z. Pilecki, R. Szermer-Zaucha, and K. Krawiec, "The Impact of High-Energy Mining-Induced Tremor in a Fault Zone on Damage to Buildings," *Energies*, vol. 14, no. 14, p. 4112, 2021, doi: 10.3390/en14144112.

[9] P. Sopata, T. Stoch, A. Wójcik, and D. Mrocheń, "Land Surface Subsidence Due to Mining-Induced Tremors in the Upper Silesian Coal Basin (Poland)—Case Study," *Remote Sens.*, vol. 12, no. 23,p. 3923, 2020, doi: 10.3390/rs12233923.

[10] K. Zhou, P. Małkowski, L. Dou, K. Yang, and Y. Chai, "Using Elastic Wave Velocity Anomaly to Predict Rockburst Hazard in Coal Mines," *Arch. Min. Sci.*, vol. 68, no. 1, pp. 141–164, 2023, doi: 10.24425/ams.2023.144322.

[11] D. Tomaszewski, J. Rapiński, L. Stolecki, and M. Śmieja, "Switching Edge Detector as a Tool for Seismic Events Detection Based on GNSS Timeseries," *Arch. Min. Sci.*, vol. 67, no. 2, pp. 317–332, 2022, doi: 10.24425/ams.2022.141461.

[12] F. Pachla and T. Tatara, "Dynamic Resistance of Residential Masonry Building with Structural Irregularities," in *Seismic Behaviour and Design of Irregular and Complex Civil Structures III*, Springer, 2020, pp. 335–347.

[13] J. Rusek, L. Słowik, and D. Rataj, "Paraseismic Resistance Evaluation for Existing Steel Conveyor Bridge Subjected to Mining Tremors," *Arch. Min. Sci.*, vol. 67, no. 4, pp. 603–630, 2022, doi: 10.24425/ams.2022.143677.

[14] A.K. Chopra, "Dynamics of structures. theory and applications to earthquake engineering," in *Earthquake Engineering*, Pearson, 2017.

[15] P. Kalisz and K. Stec, "Oddziaływanie wstrząsów górniczych na gazociągi," *Przegląd Górniczy*, vol. 72, no. 10, pp. 1–8, 2016. (in Polish)

[16] *Seismic Guidelines for Water Pipelines*. American Lifelines Alliance, 2005.

[17] S.R. Dash and S.K. Jain, "IITK-GSDMA Guidelines for seismic design of buried pipelines: provisions with commentary and explanatory examples," *Kanpur, India, National Information Center of Earthquake Engineering*, 2007.

[18] *IITK-GSDMA. Guidelines for the seismic design of buried pipelines*. Indian Institute of Technology Kanpur, 2007.

[19] D. Bekmirzaev, I. Mirzaev, R. Kishanov, N. Mansurova, and S. Sabirova, "Study of the Mass Effect of a Complex Node of UnderGround Pipelines of Orthogonal Configuration Based on Real Earthquake Records," in *Proceedings of MPCPE 2021*, 2022, pp. 371–383.

[20] H. Lu, X. Jiang, Z.-D. Xu, H. Ni, and L. Fu, "Mechanical behavior of high-pressure pipeline installed through horizontal directional drilling under seismic loads," *Tunn. Undergr. Space Technol.*, vol. 136, p. 105073, 2023, doi: 10.1016/j.tust.2023.105073.

[21] M.S. Israilov, "Action of an Oblique Seismic Wave on an Underground Pipeline," *Mech. Solids*, vol. 57, no. 5, pp. 1006–1015, 2022, doi: 10.3103/S0025654422050089.

[22] V. Calugaru, A. Nisar, C. Hitchcock, M.W. Greenfield, and R.M. Nelson, "Seismic Reliability Assessment of Buried Pipelines Subjected to Significant Permanent Ground Deformations in an M9 Cascadia Subduction Zone Earthquake," in *Lifelines 2022*, 2022, pp. 716–726.

[23] S. Toprak, E. Nacaroglu, M. Ceylan, and T.D. O'Rourke, "Effects of Ground Strain and Pipeline Orientation on Pipeline Damage during Earthquakes," in *Lifelines 2022*, 2022, pp. 489–499.

[24] D. Choudhury and C.H. Chaudhuri, "Buried Pipeline Subjected to Ground Deformation and Seismic Landslide: A State-of-the-Art Review," in *Proceedings of the 4th International Conference on Performance Based Design in Earthquake Geotechnical Engineering (Beijing 2022)*, 2022, pp. 363–375.

[25] *Guidelines for the design of buried steel pipe*. American Lifelines Alliance, 2001.

[26] M.J. O'Rourke and X. Liu, "Seismic design of buried and offshore pipelines," *MCEER Monograph MCEER-12-MN04*, p. 380, 2012.

[27] Y. Huo, S.M.M.H. Gomaa, T. Zayed, and M. Meguid, "Review of analytical methods for stress and deformation analysis of buried water pipes considering pipe-soil interaction," *Undergr. Space*, vol. 13, pp. 205–227, 2023, doi: 10.1016/j.undsp.2023.02.017.

[28] Z. Guo, J. Han, M. Hesham El Naggar, B. Hou, Z. Zhong, and X. Du, "Numerical analysis of buried pipelines response to bidirectional non-uniform seismic excitation," *Comput. Geotech.*, vol. 159, p. 105485, 2023, doi: 10.1016/j.compgeo.2023.105485.

[29] K. Zhao, N. Jiang, C. Zhou, H. Li, Z. Cai, and B. Zhu, "Dynamic behavior and failure of buried gas pipeline considering the pipe connection form subjected to blasting seismic waves," *Thin-Walled Struct.*, vol. 170, p. 108495, 2022, doi: 10.1016/j.tws.2021.108495.

[30] G. Baltzopoulos, R. Baraschino, E. Chioccarelli, P. Cito, A. Vitale, and I. Iervolino, "Near-source ground motion in the M7. 8 Gaziantep (Turkey) earthquake," *Earthq. Eng. Struct. Dyn.*, vol. 52, no. 12, pp. 3903–3912, 2023, doi: 10.1002/eqe.3939.

[31] G. Papazafeiropoulos and V. Plevris, "Kahramanmaras-Gaziantep, Turkiye Mw 7.8 Earthquake on February 6, 2023: Preliminary Report on Strong Ground Motion and Building Response Estimations," *arXiv preprint arXiv:2302.13088*, 2023.

[32] Episodes Platform, TCS AH Consortium https://episodesplatform.eu/?lang=pl#episodes:

[33] N.M. Newmark and W.J. Hall, "Pipeline design to resist large fault displacement," in *Proceedings of US National Conference on Earthquake Engineering*, 1975, vol. 1975, pp. 416–425.

[34] R. Czarny, Z. Pilecki, and D. Drzewińska, "The application of seismic interferometry for estimating a 1D S-wave velocity model with the use of mining induced seismicity," *J. Sustainable Mining*, vol. 17, no. 4, pp. 209–214, 2018, doi: 10.1016/j.jsm.2018.09.001.

[35] J. Wang and T. Tanimoto, "Estimation of Vs30 at the EarthScope Transportable Array Stations by Inversion of Low-Frequency Seismic Noise," *J. Geophys. Res.-Solid Earth*, vol. 127, no. 4, p. e2021JB023469, 2022.

[36] "IV – EQUATIONS," in *Assessment of Safety and Risk with a Microscopic Model of Detonation*, C.-O. Leiber and B. Dobratz, Eds., Amsterdam: Elsevier Science, 2003, pp. 41–78.

[37] A. Lesmana, A. Priyono, and T. Yudistira, "A Resolution Enhancement of Rayleigh Wave Dispersive Imaging using Modified Phase-Shift Method," in *IOP Conference Series: Earth and Environmental Science*, 2019, vol. 318, no. 1, p. 12019.

[38] M.J. O'Rourke, G. Castro, and I. Hossain, "Horizontal soil strain due to seismic waves," *J. Geotech. Eng.*, vol. 110, no. 9, pp. 1173–1187, 1984.

[39] M. Shinozuka and T. Koike, *Estimation of structural strains in underground lifeline pipes*. Columbia University, Department of Civil Engineering and Engineering Mechanics, 1979.

[40] INGV, ESM Engineering Strong-Motion Database, 2023. https://esm-db.eu/#/event/INT-20230206_0000008.